

# Vehicle Bridge Interaction – Extracting the dynamic characteristics of the non-stationary train passing phase

**N. Mostafa, D. Di Maio, R. Loendersloot**

University of Twente, Department of Engineering Technology,  
P.O. Box 2017, 7500AE, Enschede, The Netherlands  
e-mail: [r.loendersloot@utwente.nl](mailto:r.loendersloot@utwente.nl)

## Abstract

Monitoring of bridge has received a significant amount of attention over the past years, as the condition of these infrastructure elements is crucial to guarantee uninterrupted traffic of people and goods between regions. Most monitoring systems identify the dynamic properties of the structure, such as the resonance frequency. The resonance frequency is however not the best measure for the presence of damage. Moreover, in case the dynamics of the passing vehicle interact significantly with the dynamics of the bridge, the analysis becomes complex. Often, only the free vibration is used. Here, the Wavelet-based Synchro-Squeezed Transformation is proposed as a method to extract the instantaneous resonance frequency of the vehicle-bridge system. This allows to eliminate both operational and environmental influences. Analysis on a numerical model reveals that the method has potential to be a more robust in the identification of damage in bridge-like structure passed by a relatively heavy vehicle. A first validation based on field measurements on Irish Boyne viaduct support the capabilities of the method as predicted by the results of the numerical model.

## 1 Introduction

Monitoring of bridges has been developed and implemented on bridges over the past decades to optimise maintenance of these bridges [1]. In many cases, these monitoring systems measure the dynamic response of the bridge [2]. Among the various dynamic properties, natural frequencies can provide a simple high-level condition assessment using only a limited number of sensors, while mode shapes and their derivatives are more noise sensitive and require a higher sensor density. The free vibration of the bridge forms the base of the extraction of the modal parameters, which are influenced by the condition of the bridge, be it also by environmental conditions. This approach is suitable for many road bridges, subjected to relatively low traffic-induced excitation forces, which can be considered as a random, white noise excitation.

To avoid the non-stationary elements in the signal, the free decay signal, starting at the moment the train has left the bridge, is often used. In many cases this is sufficient to determine the main dynamic characteristics such as the natural frequencies. It is worth mentioning that the majority of the methods presented in literature using the free decay are focussing on the identification of the modal parameters, more specifically the natural frequency of a bridge.

The Hilbert-Huang Transform (HHT), combining Empirical Mode Decomposition (EMD) and the Hilbert Transform (HT), and the Continuous Wavelet Transform (CWT) are widely used for the extraction of the natural frequency of bridges. Yan and Miyamoto [3] performed a comparative study of modal parameters obtained from applying FFT, HHT and CWT to the ambient vibration response of the Z24-bridge. Similarly, He et al. [4] applied an EMD-based Random Decrement (RD) technique on the ambient vibration of the NYR steel truss bridge in China while Sayed et al. [5] applied CWT on the acceleration response of the Kaya bridge in the Seoul-Busan railway induced by a high speed train. These publications show well-separated bridge modal frequencies can be extracted from the free vibration response of bridges. The free vibration response of the Xining Beichuan bridge in China contained closely-spaced modes, which were identified by an EMD-based stochastic subspace identification technique [6].

Although the extraction of the modal parameters from the free vibration of a bridge has proven to be successful in a series of cases, there are further limitations to perform SHM based on the bridge free vibration response only. Firstly, the identified natural frequencies from the free vibration responses are dependent on the variable environmental conditions such as temperature [7]. Secondly, the extracted modal parameters using the free vibrations are actually global features which may not be sensitive to damage as a local event [8]. The vibration signal of the non-stationary part is believed to be a potentially richer part of the data: the transient change of the resonance frequencies enables elimination of environmental effects from the signal, causing deteriorating to be visible more clearly. Moreover, changes in the dynamic properties of the bridge structure due to damage may be amplified by the presence of a moving vehicle on the bridge. This requires accurate determination of the resonance frequencies in the transient part of the signal.

Railway bridges are loaded by a relatively high mass compared to their total mass, distributed over a large portion of the bridge rather than a single point. This implies that the train cannot be modelled as a moving force, but must rather be modelled as a moving mass, inherently making the vibration signal non-stationary [9]. In fact, the train should be modelled by a multi-degree of freedom spring/damper-mass system. Indeed, the vibration signal when the train traverses the bridge (Traverse Phase – TP) is a broad spectrum, noisy, non-stationary and multi-component response of a vehicle-track-bridge interacting (VBI) system. The analysis of this VBI time signal calls for advanced signal processing techniques. As for the free decay signal, continuous wavelet transformation (CWT) based methods [10, 11, 12, 13, 14, 15] or Hilbert Huang transformation (HHT) based methods [16, 17] are used for the analysis of the signal. Despite their proven strengths in analyzing non-stationary signals, these methods do show shortcomings when analyzing typical VBI signals, such as insufficient frequency resolution for the lower frequencies [9] and mode mixing for closely-spaced resonance frequencies.

The typical frequency ranges for different vibrating sub-systems in a vehicle/track system are distributed in the low frequency range, 1-10 Hz [18]. The first two bending frequencies, the most relevant for condition assessment, of a bridge structure are usually in the same frequency range. The CWT and HHT have been widely used on the Traverse Phase response for damage detection by identification of damage-induced singularities, which typically appear in a higher frequency range (i.e. well above 100 Hz) than the modal frequencies of the structure (i.e. below 10 Hz) which are of interest in this paper. This is the main reason for the insufficient frequency resolution.

The importance of including the vehicle dynamics, and the inherent complexities associated with it, are shown by the comparison of the work of Marchesiello et al. [19] on the one hand and that of Cantero et al. [20] on the other hand. The first applied CWT and short-time stochastic subspace identification (ST-SSI) on the acceleration response of a scaled bridge-like structure under a moving train without any suspension systems. The bridge time-dependent resonance was successfully extracted with both techniques. The latter applied the Wavelet transform in combination with the modified Littlewood-Paley method on the response of the Skidtrask bridge in Sweden. The proposed method was not successful in identifying the bridge resonance from the Traverse Phase response and they concluded that the dynamic interaction between the vehicle and the bridge is complex and highly dependent on the mechanical properties of the suspension systems and the distribution of the masses within the vehicle.

To overcome the issues raised in literature, the wavelet-based synchro-squeezed transformation (WSST) [21] is proposed to be used to extract the first resonance frequencies of the vehicle bridge system in the traverse phase. WSST is considered as it is reported to overcome some limitations such as mode-mixing and blurred time-frequency representations [22, 23]. This paper focusses on the use of WSST to extract the (first) resonance frequency of the vehicle-bridge combination. The objective is not to further develop the WSST method. The comparison between WSST and CWT and HHT is discussed in [24] and will not be addressed here.

Extracting the (first) resonance frequency of the traverse phase is a first step. The comparison with the (first) resonance frequency extracted from the free decay signal, allows to eliminate environmental effects. Moreover, the way the (first) resonance frequency changes during the train passage provides additional information on the condition of the bridge, independent of operational conditions such as the weight and velocity of the train.

In order to understand how WSST can be used best to extract the (first) resonance frequency, a relatively



The vehicle is created out of two nodes connected by a spring-damper element (spring stiffness  $k$  and damping  $c$ ). Point masses are attached to both nodes, representing the mass of the unsprung (wheel set,  $m_w$ ) and the sprung mass of the vehicle (bogie and body,  $m_v$ ). The mass and stiffness are chosen such that they are representative for the type of train passing the Boyne Viaduct. A velocity  $v$  in axial direction is applied to both nodes of the vehicle to ensure a stable motion. The properties of the vehicle are found in Table 2.

Table 2: Nominal properties of the vehicle used in the numerical model.

$k$ [N·m <sup>-1</sup> ]	$c$ [Ns·m <sup>-1</sup> ]	$m_v$ [kg]	$m_w$ [kg]	$f_n^{(1)}$ [Hz]
$6.40 \times 10^7$	$1.0 \times 10^4$	$54 \times 10^3$	1500	5.48

A variational study is executed to investigate the effect of variations in the stiffness and mass of the passing vehicle. In the first series, the mass and stiffness are simultaneously varied, such that the first resonance frequency of the vehicle remained constant, but the mass ratio between vehicle and bridge altered. In the second series, only the stiffness is varied, resulting in a changing frequency ratio between the first natural frequencies of the bridge and vehicle. The list of cases is found in Table 3.

Table 3: Varying mass and stiffness and resulting mass and resonance frequency ratio.

	Case 1					Case 2				
	$m_v$	$k$	$f_n^{(1)}$	$\alpha_m$	$\alpha_f$	$m_v$	$k$	$f_n^{(1)}$	$\alpha_m$	$\alpha_f$
1	$54 \times 10^3$	$6.40 \times 10^7$	5.48	0.21	1.87	$54 \times 10^3$	$1.92 \times 10^7$	3.00	0.21	1.02
2	$40 \times 10^3$	$4.74 \times 10^7$	5.48	0.16	1.87	$54 \times 10^3$	$2.24 \times 10^7$	3.24	0.21	1.11
3	$42 \times 10^3$	$4.98 \times 10^7$	5.48	0.17	1.87	$54 \times 10^3$	$2.56 \times 10^7$	3.47	0.21	1.18
4	$44 \times 10^3$	$5.21 \times 10^7$	5.48	0.17	1.87	$54 \times 10^3$	$2.88 \times 10^7$	3.68	0.21	1.26
5	$46 \times 10^3$	$5.45 \times 10^7$	5.48	0.18	1.87	$54 \times 10^3$	$3.20 \times 10^7$	3.87	0.21	1.32
6	$48 \times 10^3$	$5.69 \times 10^7$	5.48	0.19	1.87	$54 \times 10^3$	$3.52 \times 10^7$	4.06	0.21	1.39
7	$50 \times 10^3$	$5.93 \times 10^7$	5.48	0.20	1.87	$54 \times 10^3$	$3.84 \times 10^7$	4.24	0.21	1.45
8	$52 \times 10^3$	$6.16 \times 10^7$	5.48	0.21	1.87	$54 \times 10^3$	$4.16 \times 10^7$	4.42	0.21	1.51
9	$56 \times 10^3$	$6.64 \times 10^7$	5.48	0.22	1.87	$54 \times 10^3$	$4.48 \times 10^7$	4.58	0.21	1.57
10	$58 \times 10^3$	$6.87 \times 10^7$	5.48	0.23	1.87	$54 \times 10^3$	$4.80 \times 10^7$	4.75	0.21	1.62
11	$60 \times 10^3$	$7.11 \times 10^7$	5.48	0.24	1.87	$54 \times 10^3$	$5.12 \times 10^7$	4.90	0.21	1.67
12	$62 \times 10^3$	$7.35 \times 10^7$	5.48	0.25	1.87	$54 \times 10^3$	$5.44 \times 10^7$	5.05	0.21	1.72
13	$64 \times 10^3$	$7.59 \times 10^7$	5.48	0.25	1.87	$54 \times 10^3$	$5.76 \times 10^7$	5.20	0.21	1.77
14	$66 \times 10^3$	$7.82 \times 10^7$	5.48	0.26	1.87	$54 \times 10^3$	$6.08 \times 10^7$	5.34	0.21	1.82
15						$54 \times 10^3$	$6.40 \times 10^7$	5.48	0.21	1.87
16						$54 \times 10^3$	$6.72 \times 10^7$	5.61	0.21	1.92
17						$54 \times 10^3$	$7.04 \times 10^7$	5.75	0.21	1.96
18						$54 \times 10^3$	$7.36 \times 10^7$	5.88	0.21	2.01

Next to the variations on stiffness and the mass of the vehicle, a number of simulations is done with a local or global stiffness reduction. Damage is mimicked by reducing the stiffness of a series of elements by 10% (by assigning material with a lower Young's modulus). Secondly, the stiffness of all elements is reduced by 10%, similar to a change in environmental conditions, be it a reduction of 10% is quite significant, and a more realistic situation would be a distribution of stiffness due to for example heating of one side of the construction by the sun. The following cases were observed:

1. Stiffness reduction of 10 elements (0.5 m) centered around mid-span
2. Stiffness reduction of 20 elements (1.0 m) centered around mid-span

### 3. Global stiffness reduction

The results of these cases are compared against the baseline numerical model. At this point, the variation in damage cases is still limited. However, the purpose is to analyse the way the instantaneous first resonance frequency changes.

## 3 Field measurements

The Boyne viaduct, a single track railway bridge as it exists today, was constructed in the early 1930s and consists of 15 semi-circular masonry arch spans and three simply supported steel-girder spans (Figure 2). The central steel-girder span is approximately 81m long and has been instrumented with accelerometers and strain gauges. The strain gauges data have been used for the response phase separation and identifying the first and the last sample of the Traverse Phase. The data from the accelerometer installed at the mid-span of the bridge has mainly been used for the bridge health monitoring. The sampling frequency of the measurements is 2 kHz. The bridge fundamental frequency, 2.9 Hz, is obtained by a frequency analysis of the bridge free vibration.



Figure 2: The Boyne viaduct railway bridge in Drogheda, Ireland.

A limited variation of train types passes the Boyne viaduct: a “Diesel Multiple Unit” (DMU) train, consisting of 4 to 9 carriages, each having its own diesel engine; and an “Enterprise” train, consisting of a locomotive and a series of carriages. Approximately 20 train passages per day were measured over a period covering two years, resulting in an extensive amount of field measurement data. Next to the regular train type, two types of signals are identified for two types of single vehicles crossing the bridge: a single locomotive and a maintenance train. These are the most basic examples of vehicles passing the bridge, corresponding closest to the numerical case, and will therefore be analysed first.

## 4 Results & discussion

### 4.1 Numerical model - without damage

The WSST is applied to the acceleration data retrieved from the numerical model. At first, only the vertical acceleration of the center node of the bridge is used. A ‘bump’ mother wavelet is used. The transformed signal of the baseline simulation is shown in Figure 3. The first figure shows the full spectrum, hence the colour indicates the amplitude of the signal at each frequency and time. The second figure only shows at which frequency the maximum amplitude is found for each time step: the first instantaneous resonance

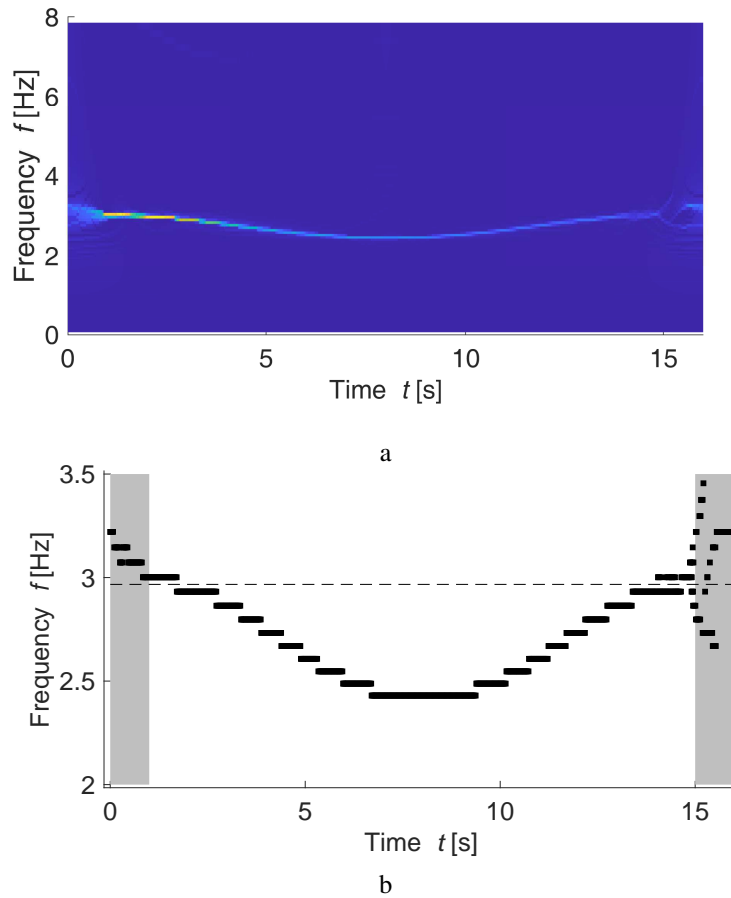


Figure 3: Time-frequency response extracted by WSST of the acceleration of the bridge mid-node of the baseline numerical simulation. (a) Full spectrum; (b) maximum in the spectrum; dashed line: resonance frequency from the leaving phase.

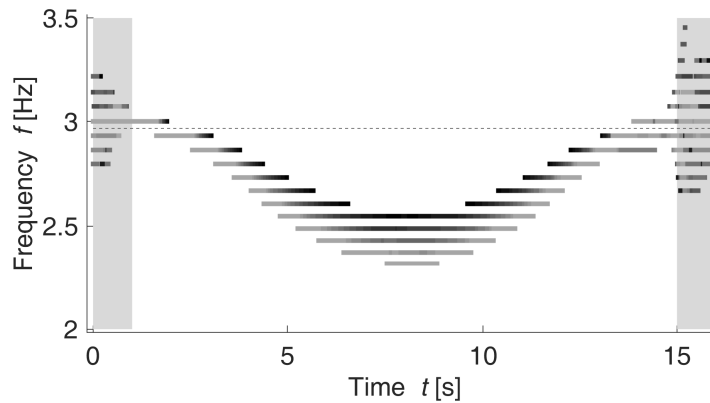
frequency of the vehicle bridge system. The dashed line equals the first resonance frequency as extracted from the leaving phase.

It is known that WSST can give somewhat distorted results at both tails of the signal, explaining the slightly more blurry spectrum in the first and the last second of the traverse signal. These areas are indicated in the graphs in Figure 3(b) by the gray colour. These areas may be omitted from further analysis.

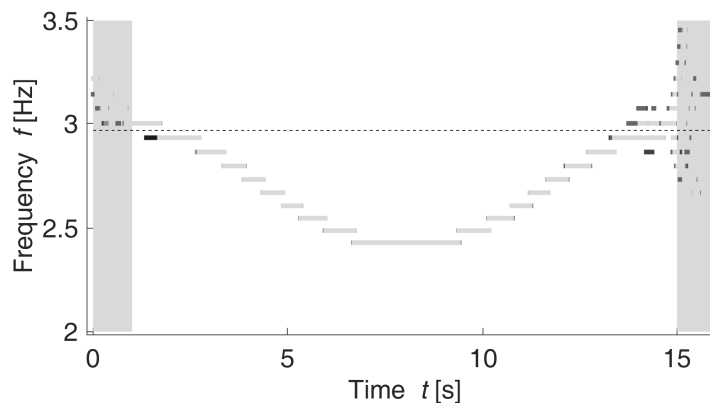
The second resonance frequency of the bridge-vehicle system is not visible in the time-frequency spectrum, as it is not, or only weakly, activated. Typically, the resonance frequency ratio between vehicle and bridge should be close to unity and the mass ratio should be sufficiently high to see a significant amplitude of this second resonance frequency. In a field situation, the stiffness characteristic of the train and its weight compared to those properties of the bridge will determine the presence of secondary resonance frequencies of the vehicle-bridge system.

The instantaneous first resonance frequency starts and ends at the bridge resonance frequency, as is expected: the spring mass does not influence the resonance frequency of the bridge at the start and end, simply because it either is about to enter the bridge or has just left it. However, as the mass progresses over the bridge, the added mass (approximately 21% of the bridge mass) causes the resonance frequency of the combined system to drop. As shown by Mostafa et al. [24], this corresponds to the behaviour observed when executing a series of eigen frequency analysis with the mass positioned at different position of the bridge. Evidently, such an analysis is not possible in an operational condition, but field tests of a similar kind have been reported in the literature.

Changing the mass and the stiffness, such that the resonance frequency of the vehicle remains constant (the first variational study), reveals an increased drop in the instantaneous frequency, see Figure 4(a). The importance of this graph is the single dashed line, implying that in all cases, the same frequency was found in the leaving phase of the signal – which is to be expected and not more than a confirmation of a correct numerical implementation of the problem.



a



b

Figure 4: Instantaneous first resonance frequency of the bridge-vehicle system. (a) Increasing mass ratio of the vehicle and bridge. Dark to light refers to low to high mass ratio. (b) Increasing resonance ratio of the vehicle and bridge. Dark to light refers to low to high frequency ratio.

Changing the stiffness, without changing the mass, leads to a variation in the stiffness ratio. The results are not affected by the changing mass ratio (see Figure 4(b)). This is according to the expectation, although a second instantaneous resonance frequency was expected. The absence of this second instantaneous resonance frequency is most likely attributed to a combination of mass ratio, frequency ratio and settings in the numerical model.

## 4.2 Numerical model - with damage

Changing the stiffness of a small number of elements, results in change in the response which is strongest as the vehicle passes the section with reduced stiffness. This is expected to be reflected in a difference in

the pattern of the instantaneous resonance frequency. As seen earlier, the instantaneous resonance frequency changes smoothly, but in case of damage it is expected to show a less smooth pattern.

Firstly, the cases with 10 and 20 elements (0.5 m and 1.0 m respectively) with a 10% stiffness reduction are analysed. The instantaneous resonance frequencies are depicted in Figure 5. The first observation is that the stiffness reduction over 10 elements does, in the given situation, not yield any noticeable difference. It should be noted the effect on the global dynamic properties in this situation is small: the resonance frequency of the bridge changes much less than 1%. In addition, the vehicle is only a point mass and passes the section with reduced stiffness over a short period of time.

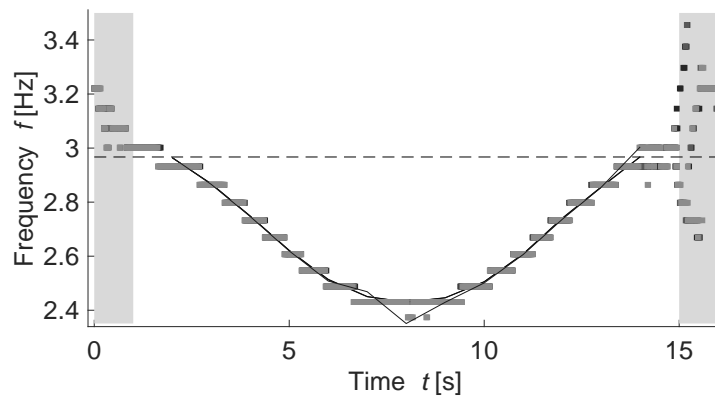


Figure 5: Instantaneous first resonance frequency of the bridge-vehicle system without damage and with 10 and 20 elements with reduced stiffness. Dark to light refers to none to 20 elements stiffness reduction. The drawn lines are spline fits.

The second observation, however, is that the results of the case with 20 elements with reduced stiffness, does show a different pattern. It may not be visible immediately, as the frequency resolution is relatively limited. However, the sections in which the instantaneous resonance frequency remains constant, are slightly different. A spline is fit through the center of these sections of constant instantaneous resonance frequency, more clearly revealing the small, yet noticeable difference. It should be noted that the change of resonance frequency of the bridge is still well below 1%. This approach can therefore be considered as a significant improvement regarding the capability of identifying the presence of damage.

### 4.3 Numerical model - environmental change

Finally, the case with 20 elements with reduced stiffness and that with a global stiffness reduction are compared against the baseline model (see Figure 6). The graphs show that the global stiffness reduction simply lowers the instantaneous resonance frequency. In other words: the patterns remains the same as for the baseline case. This in contrast to the case with damage. Moreover, the resonance frequency of the bridge can be acquired from the leaving phase, as was shown earlier, hence, one could normalize the graphs based on the measured resonance frequency in the leaving phase. This eliminates changes due to environmental effects that affect the global resonance frequencies.

A possible measure for the presence of damage is based on a comparison between the patterns observed in the instantaneous resonance frequency. This is a potentially significantly more robust measure than for example the change of the resonance frequency. It can be argued that also mode shapes, or their derivatives are a stronger measure than the change of resonance frequency, but this requires more sensors. The method presented here, relies on the use of a single sensor.

### 4.4 Field measurements

The two train analysed in this case are selected because they best approximate a single sprung mass moving over the bridge. Limited information is available on these trains: only the weight of the 201 Class locomotive



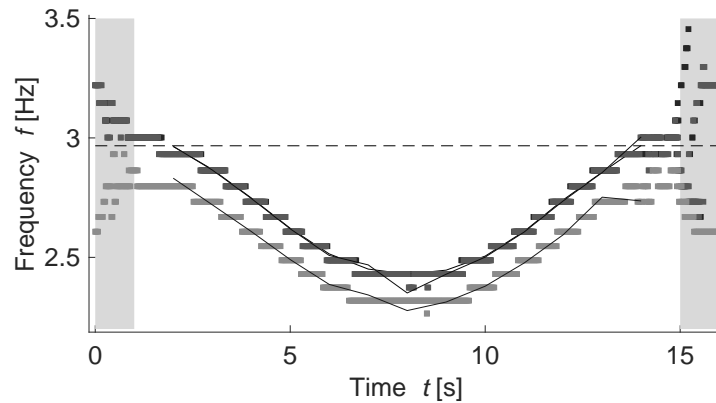


Figure 6: Instantaneous first resonance frequency of the bridge-vehicle system without damage, with 20 elements with reduced stiffness and with a global stiffness reduction. The lighter gray line corresponds with the model with global stiffness reduction.

is known (112.5 ton), which is about 20% of the weight of the Boyne viaduct and therefore similar to the mass ratio for the baseline numerical model. The frequency spectrum and the instantaneous first resonance frequency for the single locomotive is shown in Figure 7. The data used for the analysis is the acceleration in vertical direction of the triaxial accelerometer position at mid-span of the bridge. The strain gauge data of strain gauges close to the center span and close to the bridge head are used to determine the velocity of the train, which is subsequently used to determine the start and end of the traverse phase.

Despite a significantly more noisy signal, to which no additional filtering is applied, a clear change of the resonance frequency during passage of the train can be observed. The results suggest that the train is short compared to the bridge, or at least has a relative short distance between the wheels, resulting in a localised load.

The maintenance train shows a different characteristic, which is attributed to different characteristics, such as the weight, stiffness of the suspension, wheel base etc. The resonance frequency lowers more quickly, to then stay at a constant value for some time. This suggest a relatively large distance between the load point (hence a large wheel base). Some indication of a second resonance frequency are also visible (around 2 seconds).

## 4.5 Discussion

The importance of these results is that each train has its own signature. Hence, one of the first steps in the analysis of field data is the identification of the different train types. The time-frequency signal is also influenced by operational conditions such as the weight of the train and its velocity. However, the weight of the train will not change the shape of the pattern, but only the amplitude, as is suggested by the numerical results. Environmental effects do also influence the time-frequency signal, but only causes a shift. Focussing on the pattern, one can conclude that knowing the pattern in detail, will allow for a robust anomaly identification, relatively independent of environmental and operational conditions. It is essential to be able to extract the instantaneous first resonance frequency accurately. The results presented here show that the WSST is a promising method for this.

Evidently, the model needs further validation. Currently, simulation are being analysed of more complex vehicle, including not just primary, but also secondary suspension. In addition, multiple units of these vehicles are coupled, providing a more realistic representation of the a train passage. Next to that, experiments with a single sprung mass rolling over a flexible beam were scheduled to more fundamentally support the concept of using WSST for damage identification. However, these are momentarily postponed, due to Covid-19 related restriction on laboratory work.

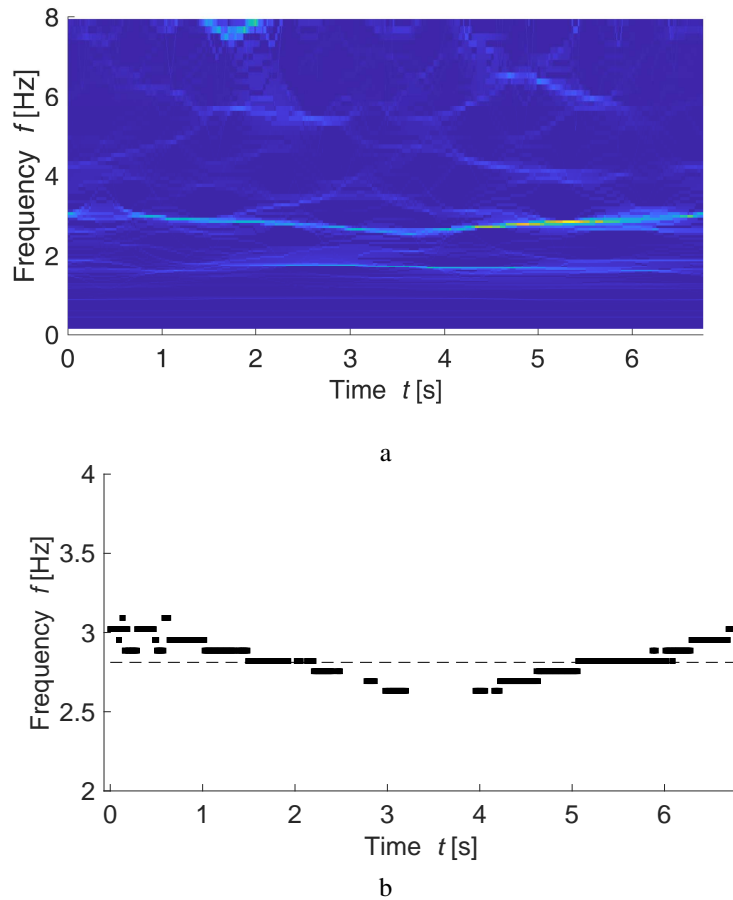


Figure 7: Time-frequency response extracted by WSST of the acceleration measured at the bridge mid-span accelerometer of the passage of a single 201 Class locomotive. (a) Full spectrum; (b) Maximum in the spectrum; dashed line: resonance frequency from the leaving phase.

## 5 Conclusions & recommendations

The Wavelet-based Synchro-Squeezed Transformation (WSST) is proposed as a method to improve the damage identification of bridge like structures with a vehicle strongly interacting with the structure it passes. Although the work presented here is based on a relatively basic model, a number of conclusions can be drawn:

- The damage identification based on the pattern of the first instantaneous resonance frequency is possible with WSST, thanks to the sufficiently high frequency resolution at low frequencies;
- Operational conditions, such as the weight and the dynamics of the passing vehicle do not affect the pattern of the instantaneous resonance frequency and can hence be eliminated from the damage identification process;
- Environmental conditions, globally changing the bridge dynamic properties can be eliminated, as the pattern of the instantaneous resonance frequency is not changed, only shifted vertically. The pattern can be normalized with the resonance frequency retrieved from the leaving phase, eliminating the vertical shift.

Of course, the validity of these conclusions only stretch the numerical model presented here. The following activities are currently being executed or will be in the near future:

- An experimental set-up will be realized to measure the effect of sprung mass systems on beam like

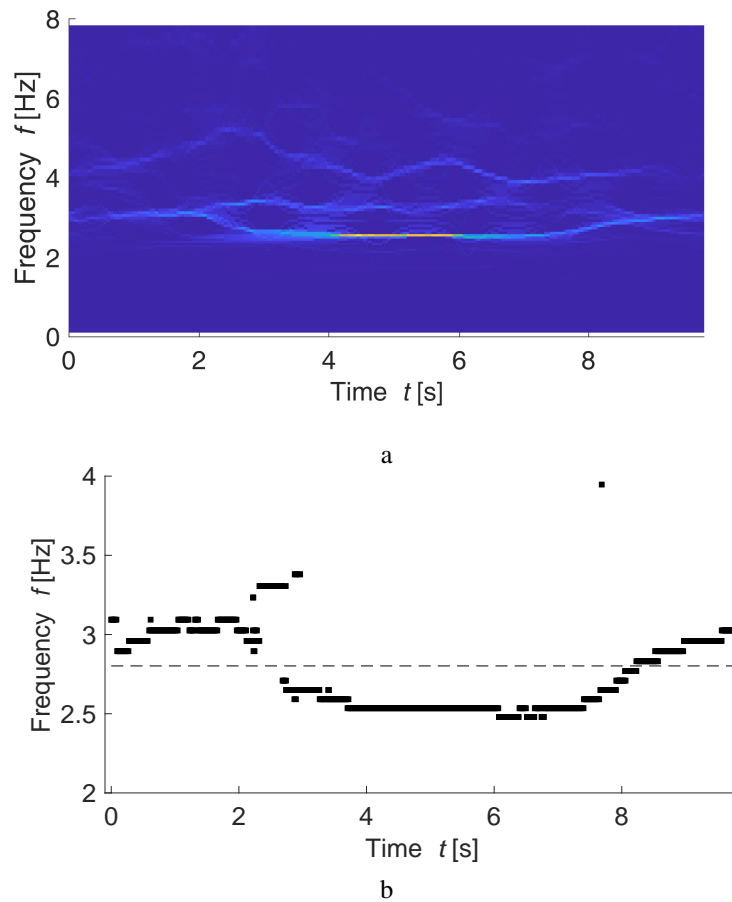


Figure 8: Time-frequency response extracted by WSST of the acceleration measured at the bridge mid-span accelerometer of the passage of a maintenance train. (a) Full spectrum; (b) maximum in the spectrum; dashed line: resonance frequency from the leaving phase.

structures to gain more understanding of the factor affecting the results as measured in field measurements. Covid-19 restrictions have delayed this activity;

- More complex vehicles are added to the numerical model, corresponding to the trains – in terms of dynamics – that pass the Boyne viaduct. The simulations of these cases are currently running and being analysed;
- A detailed analysis of the field data acquired from two years of measurements on the Boyne viaduct is currently being done in parallel, to validate the proposed method and assess how it can be used best in a realistic case.

## Acknowledgements

This study has been performed as part of the DESTination RAIL project — Decision Support Tool for Rail Infrastructure Managers. This project has received funding from the European Union's Horizon 2020 research and innovation program under grant agreement No 636285.

## References

- [1] D. Frangopol, Y. Dong, and S. Sabatino, "Bridge life-cycle performance and cost: analysis, prediction, optimisation and decision-making," *Structure and Infrastructure Engineering*, vol. 13, pp. 1239–1257, 2017.
- [2] J. Casas and J. Moughty, "Bridge damage detection based on vibration data: past and new developments," *Frontiers in Built Environment*, vol. 3, pp. 1–12, 2017.
- [3] B. Yan and A. Miyamoto, "A comparative study of modal parameter identification based on wavelet and hilbert-huang transforms," *Computer-Aided Civil and Infrastructure Engineering*, vol. 21, pp. 9–23, 2006.
- [4] X. He, X. Hua, Z. Chen, and F. Huang, "Emd-based random decrement technique for modal parameter identification of an existing railway bridge," *Engineering Structures*, vol. 33, pp. 1348–1356, 2011.
- [5] M. Sayed, M. Kaloop, E. Kim, and D. Kim, "Assessment of acceleration responses of a railway bridge using wavelet analysis," *KSCE Journal of Civil Engineering*, vol. 21, pp. 1844–1853, 2017.
- [6] D. Yu and W. Ren, "Emd-based stochastic subspace identification of structures from operational vibration measurements," *Engineering Structures*, vol. 27, pp. 1741–1751, 2005.
- [7] J. Moughty and J. Casas, "A state of the art review of modal-based damage detection in bridges: Development, challenges, and solutions," *Applied Sciences*, vol. 7, p. 24, 2017.
- [8] J. Chen, "Application of empirical mode decomposition in structural health monitoring: Some experience," *Advances in Adaptive Data Analysis*, vol. 1, pp. 601–621, 2009.
- [9] J. Li, X. Zhu, S. seong Law, and B. Samali, "Time-varying characteristics of bridges under the passage of vehicles using synchroextracting transform," *Mechanical Systems and Signal Processing*, vol. 140, p. 106727, 2020. [Online]. Available: <https://doi.org/10.1016/j.ymsp.2020.106727>
- [10] W. He and S. Zhu, "Moving load-induced response of damaged beam and its application in damage localization," *Journal of Vibration of Control*, vol. 22, pp. 3601–3617, 2016.
- [11] A. Khorram, M. Rezaeian, and F. Bakhtiari-Nejad, "Multiple cracks detection in a beam subjected to a moving load using wavelet analysis combined with factorial design," *European Journal of Mechanics, A/Solids*, vol. 40, pp. 97–113, 2013. [Online]. Available: <http://dx.doi.org/10.1016/j.euromechsol.2012.12.012>
- [12] W. Zhang, J. Li, H. Hao, and H. Ma, "Damage detection in bridge structures under moving loads with phase trajectory change of multi-type vibration measurements," *Mechanical Systems and Signal Processing*, vol. 87, pp. 410–425, 2017. [Online]. Available: <http://dx.doi.org/10.1016/j.ymsp.2016.10.035>
- [13] V. Pakrashi, A. O'Connor, and B. Basu, "A bridge-vehicle interaction based experimental investigation of damage evolution," *Structural Health Monitoring*, vol. 9, pp. 285–296, 2010.
- [14] D. Hester and A. González, "A wavelet-based damage detection algorithm based on bridge acceleration response to a vehicle," *Mechanical Systems and Signal Processing*, vol. 28, pp. 145–166, 2012.
- [15] A. González and D. Hester, "An investigation into the acceleration response of a damaged beam-type structure to a moving force," *Journal of Sound and Vibration*, vol. 332, pp. 3201–3217, 2013.
- [16] J. Meredith, A. González, and D. Hester, "Empirical mode decomposition of the acceleration response of a prismatic beam subject to a moving load to identify multiple damage locations," *Shock and Vibration*, vol. 19, pp. 845–856, 2012.

- [17] H. Aied, A. González, and D. Cantero, "Identification of sudden stiffness changes in the acceleration response of a bridge to moving loads using ensemble empirical mode decomposition," *Mechanical Systems and Signal Processing*, vol. 66-67, pp. 314–338, 2016. [Online]. Available: <http://dx.doi.org/10.1016/j.ymssp.2015.05.027>
- [18] D. Connolly, G. Kouroussis, O. Laghrouche, C. Ho, and M. Forde, "Benchmarking railway vibrations - track, vehicle, ground and building effects," *Construction and Building Materials*, vol. 92, pp. 64–81, 2015.
- [19] S. Marchesiello, S. Bedaoui, L. Garibaldi, and P. Argoul, "Time-dependent identification of a bridge-like structure with crossing loads," *Mechanical Systems and Signal Processing*, vol. 23, pp. 2019–2028, 2009.
- [20] D. Cantero, M. Ülker-Kaustell, and R. Karoumi, "Time-frequency analysis of railway bridge response in forced vibration," *Mechanical Systems and Signal Processing*, vol. 76-77, pp. 518–530, 2016. [Online]. Available: <http://dx.doi.org/10.1016/j.ymssp.2016.01.016>
- [21] I. Daubechies, J. Lu, and H. Wu, "Synchrosqueezed wavelet transforms: An empirical mode decomposition-like tool," *Applied and Computational Harmonic Analysis*, vol. 30, pp. 243–261, 2011. [Online]. Available: <http://dx.doi.org/10.1016/j.acha.2010.08.002>
- [22] H. Wu, P. Flandrin, and I. Daubechies, "One or two frequencies? the synchrosqueezing answers," *Advances in Adaptive Data Analysis*, vol. 3, pp. 29–39, 2011.
- [23] Q. Jiang and B. Suter, "Instantaneous frequency estimation based on synchrosqueezing wavelet transform," *Signal Processing*, vol. 138, pp. 167–181, 2017.
- [24] N. Mostafa, D. Di Maio, and R. Loendersloot, "Extracting the time-dependent resonances of a vehicle-bridge interacting system by wavelet synchrosqueezed transform," *Structural Control and Health Monitoring*, vol. 0, p. submitted, 2020.
- [25] R. Loendersloot and N. Mostafa, "Failure modes & mechanisms and bridge monitoring systems," University of Twente, Deliverable D1.5, 2018, <http://www.destinationrail.eu/ajax/DownloadHandler.php?file=2136>.